Spectroscopic and selected mechanical properties of diamond-like carbon films synthesized by broad-beam ion deposition from methane

C. V. Cooper
United Technologies Research Center, 411 Silver Lane, East Hartford, CT 06106 (USA)

C. P. Beetz, Jr.,
Advanced Technology Materials, 7 Commerce Drive, Danbury, CT 06810 (USA)

B. W. Buchholtz, P. J. Wilbur and R. Wei
Colorado State University, Fort Collins, CO 80523 (USA)

Abstract

Broad-beam ion deposition was employed to decompose methane for the synthesis of diamond-like-carbon (DLC or a-C:H) films, deposited to two thicknesses of approximately 1 and 5 μm, onto AISI M50 substrates in the presence or absence of a submicrometer intermediate layer of either amorphous Si:C:H or elemental Si. During deposition from CH_4, the current density supplied to the ion gun was maintained at a constant 2.5 mA cm^{-2}, while the accelerating potential was varied over the range 250–700 eV. The resulting microstructures, characterized using scanning electron microscopy and stylus-type profilometry, revealed ultrasmooth and essentially featureless surfaces for all films. Raman spectroscopy produced spectra which could be deconvoluted most effectively by the superposition of peaks positioned at three wavenumbers, predominated by the peak ascribable to sp^2-hybridized bonding; it was, however, unable to differentiate from among the films deposited at various ion-beam energies. Fourier-transform IR (FTIR) reflectivity revealed that the ratio of sp^3 to sp^2 carbon-bonded hydrogen in the films was approximately 3.5; FTIR results exhibited a modest trend toward decreasing sp^3 to sp^2 ratio for films deposited with increasing ion-beam energy. Nanoindentation properties of hardness and elastic modulus were found to be essentially insensitive to ion accelerating energy; however, adherence between the film and mechanically polished M50 substrate as measured by the scratch technique displayed a modest dependence on accelerating energy, with a maximum critical force occurring for films deposited at the highest energy investigated, 677 eV. Conversely, an inverse relationship between friction coefficient and ion deposition energy emerged, with coefficients ranging between 0.105 and 0.153. The film grown to a thickness of approximately 5 μm exhibited decidedly inferior adherence to the M50 substrate than those grown to a thickness of approximately 1 μm. Deposition at an energy of 260 eV onto the elemental Si intermediate layer or deposition directly onto the M50 substrate in the absence of an intermediate layer failed to produce adherent films, spalling spontaneously either immediately or within days following deposition.

1. Introduction

Diamond-like-carbon (DLC) coatings and thin films possess many attractive properties of engineering importance, including high hardness, optical transparency over a wide range of wavelengths [1], good thermal conductivity, good environmental resistance [1], for example to aqueous corrosion, and good solid lubricity, the last of which is believed to be related to the presence or transformation to the graphitic (hexagonal) phase of carbon [2], the formation of a transfer layer on the non-DLC-coated counterbody [3–6], and the presence of hydrogen [7]. Of not such an attractive character, DLC coatings, which are synthesized principally by physical vapor deposition (PVD) rather than the chemical vapor deposition (CVD) techniques employed to synthesize the fully crystalline counterpart, typically exhibit high internal stresses [8–10] and commonly incorporate hydrogen concentrations as high as 60% [11], which may reduce its hardness and is likely to increase its coefficient of thermal expansion. In addition to high hardness levels and low coefficient of friction values, DLC coatings deposited by broad-beam ion deposition have been reported to exhibit greatly improved rolling-contact-fatigue (RCF) lifetimes at extremely high contact stresses compared with the performance of baseline (uncoated) bearing alloys such as AISI M50, AISI 440C, AISI 52100, and the surface-carburizing alloy AISI 4118 [12, 13].

A relatively understudied but, from an engineering standpoint, vitally important characteristic of any coating, including those composed of DLC, is its ability to adhere to the substrate onto which it is deposited. Interestingly, it has been reported that the adherence of ion-beam-synthesized DLC coatings to the wrought, artificially aged aluminum alloy 6061-T6 showed a

0925–9635/94/$7.00

SSDI 0925-9635(93)05082-N

strong dependence on ion-beam energy during deposition [14], with an optimal deposition energy being found to be approximately 450 eV. To our knowledge, a systematic study of this type to determine such behavior has not been attempted and reported for ferrous alloys. The objective of this paper is a determination of the microstructure and spectroscopic and selected mechanical properties of DLC films, deposited from methane via broad-beam ion techniques onto M50 substrates, and systematic changes in the latter which are caused by parametric variations in ion deposition energy.

2. Experimental details

2.1. Deposition and microstructural characterization

Throughout this study, films have been deposited onto substrates composed of quenched and tempered, vacuum-induction-melted/vacuum-arc-remelted (VIM/VAR) AISI M50, having a composition, weight per cent, of 0.80 C, 0.30 Mn, 0.20 Si, 4.00 Cr, 1.00 V, 4.25 Mo, and balance Fe. Prior to deposition, all substrates were machined to dimensions of 28.6 mm in diameter by 3.2 mm thick and were heat treated as follows: (a) preheated to 843 °C for 0.25 h, (b) solutionized at 1121 °C in vacuum for 0.5 h, (c) oil-quenched to 22 °C, and (d) double-tempered at 566 °C for 2 h. The resulting microstructure consisted of tempered martensite, and the measured hardness was R_C 61.6. The specimens were surface and hand ground following tempering and mechanically polished through 1 μm diamond compound, producing an arithmetic-average surface roughness R_a of approximately 10 nm. Following mechanical polishing, M50 disc coupons were degreased ultrasonically in 1,1,1-trichloroethane, acetone, and methanol in sequence for 180 s each.

Thereafter, coupons were placed in the working chamber of the ion-deposition system and evacuated to a base pressure of approximately 3.3×10^{-3} Pa (2.5×10^{-5} Torr); Ar gas was supplied to the 10 cm diameter Kaufman-type ion gun for the purpose of sputter cleaning the M50 substrates. Singly ionized Ar was accelerated towards the M50 coupons for 180 s at an energy of 1.0 keV and a beam current density of approximately 2.5 mA cm^{-2}. Similarly, an Si target was Ar^+ sputter cleaned for a period of 300 s. Subsequent to sputter cleaning, an intermediate layer of elemental Si or a compound layer of amorphous Si:C:H was deposited onto the M50 substrates, the former in an evacuated chamber and the latter in a chamber backfilled with CH_4 and Ar to partial pressures of 2×10^{-2} and 5.3×10^{-2} Pa (1.5×10^{-4} and 4.0×10^{-4} Torr) respectively. For both compositions, the interlayer was grown to a thickness of approximately 130 nm. Finally, DLC films were synthesized on the M50 substrates to thicknesses of approximately 1 μm, and in one case 5 μm, using an evacuated chamber by supplying CH_4 to the ion gun. Deposition experiments were conducted at discrete accelerating energies of 260, 350, 466, 570, and 677 eV at a constant current density of 2.5 mA cm^{-2}. During all phases of sputter cleaning and deposition, substrates were maintained at a temperature of approximately 100 °C via water cooling.

Microstructural characterization was accomplished using a Cambridge model Stereoscan 250 and an Amray model 1850 FE field-emission microscope operating at an electron potential of 2 or 20 kV, both equipped with energy-dispersive X-ray analysis spectrometers. Surface roughness was determined using a contacting-type surface profilometer, Veeco Dektak model 3030, using a diamond stylus with a tip radius of curvature of 12.5 μm.

2.2. Spectroscopic characterization

IR reflection spectroscopy was used to characterize the DLC films and to detect the presence of sp^2 and sp^3 carbon species which have strong C–H stretching absorption bands in the 3300–2850 cm^{-1} region. IR reflection measurements were taken on a Perkin Elmer model 1600 Fourier transform IR (FTIR) spectrometer. In addition, Raman spectroscopy was used to characterize the DLC films. Grazing incidence, laser-excited Raman spectra were taken from the surface of the deposited films to assess the bonding characteristics of the DLC films. The Raman spectra were collected using a SPEX model 1403, 0.85 m double-pass monochrometer with 1800 gr mm^{-1} holographic gratings. A Hamamatsu R943-02 photomultiplier was used for single-photon counting; the detector dark current was approximately 3 cps. The Raman spectra were excited using the 488.0 nm line of an Ar^+ ion laser, Lexel model 95.

2.3. Ultralow-load indentation

Ultralow-load indentation experiments were conducted using a Nano Instruments Corporation model Nanoindenter I. For these experiments, a Berkovich-type (three-sided pyramid), type Ia diamond indenter [15], having a carefully calibrated area function, was loaded against the DLC coating at loading and unloading rates of 100 μN s^{-1} to a maximum total indentation depth of 100 nm; following loading to 100 nm depth, a 10 s dwell at maximum load was incorporated prior to unloading. This indenter geometry facilitates easy conversion to and from Vickers values through the relation $\sigma_V = 0.927\sigma_N$ [16], where σ_V and σ_N are the indentation stress (hardness) associated with the Vickers and nanoindenter measurements respectively. As the thickness of DLC films was as small as 1.0 μm, an indentation depth of 100 nm was chosen in an effort to avoid contributions from the M50 substrate [17, 18]. As described by other

researchers [19], the contribution from elastic deformation has been subtracted from the total indentation depth before computation of the hardness, such that reported values of hardness reflect the resistance of the DLC films to plastic flow only.

A two-dimensional array of indent loci was programmed for automated execution by the nanoindenter with a spacing between indents of 20 μm. Values for the elastic modulus were determined by fitting the initial unloading portion of the load–displacement curve using a linear-least-squares approach in conjunction with the calibrated area function. Additional details regarding the application of nanoindentation to determine hardness and elastic modulus of thin films, including those composed of DLC, may be found elsewhere [19, 20].

2.4. Adhesion

Adhesion measurements have been taken during the course of this study on DLC-coated specimens. For these experiments, an instrument manufactured by CSEM, model MST [21], was employed. This device utilizes a sharp, Rockwell "C" indenting diamond having a tip radius of curvature of 200 μm. For the purposes of this study, a progressively increasing load ranging from 0 to 30 N was applied to the diamond indenter at a rate of 0.5 N s^{-1} as the DLC-coated specimen was translated at a rate of 0.167 mm s^{-1}, resulting in a specific loading rate of 3 N mm^{-1}. This and similar instruments have been employed effectively to produce semi-quantitative comparisons of adherence between thin, hard and ultra-hard coatings and metallic substrates of widely varying compositions [21–23].

This study has employed a series of four parallel scratch traverses at a spacing of 0.5 mm. The device is instrumented with sensors to measure acoustic energy and tangential (frictional) force during translation. Acoustic emission and post-scratch light microscopy were utilized to determine the critical forces, L_c(AE) and L_c(LM) respectively, defined to be the force required to initiate incipient film failure. It has been reported [24] that stylus damage, including blunting, can lead to dramatic decreases in measured critical forces. To confirm the avoidance of such extraneous influences, the stylus tip was inspected using light microscopy at the conclusion of each DLC specimen (four scratch traverses); these periodic inspections demonstrated that the stylus was completely free from damage.

2.5. Sliding wear

Sliding wear experiments of an oscillatory pin-on-disc type [25] were performed without lubrication on specimens which were cleaned thoroughly with organic solvents as described above. For these, a highly polished ball of 4.8 mm diameter composed of ruby (Cr-doped) sapphire was loaded against the rotating, DLC-coated coupon at a rotational speed of 1.33 s^{-1}, which resulted in a linear speed of 0.12 m s^{-1}. Contact stresses of 2.17, 2.42, 2.67, 2.92, and 3.17 GPa, corresponding to loads of 44.6, 61.3, 82.3, 107.7, and 137.8 N respectively, were applied sequentially through the ruby sapphire ball to the DLC-coated disc for 4800 passes at each stress level. All sliding wear experiments were performed in laboratory air of approximately 35% relative humidity.

3. Results and discussion

3.1. Deposition and microstructure

A summary of the deposition experiments is presented in Table 1. All deposition conditions resulted in the synthesis of adherent DLC films except for specimen numbers 1 and 7, the former of which was deposited onto an elemental Si interlayer at the lowest investigated beam energy of 266 eV and the latter of which was

TABLE 1. Deposition, indentation, and adhesion of a-C:H films on AISI M50 substrates

Specimen number	Interlayer composition	Deposition energy (eV)	Approximate film thickness (μm)	Indentation hardness (GPa)	Indentation modulus (GPa)	Critical load, L_c(LM) (N)	Critical load L_c(AE) (N)
1	Si	260	1.0	NA	NA	0	0
9, 10	Si	350	1.0	11.64 ± 0.23	87.5 ± 1.6	19	23
2, 11, 12	Si	466	1.0	10.42 ± 0.69	75.0 ± 4.1	21	20
13, 14	Si	570	1.0	9.51 ± 0.75	69.3 ± 5.7	16	16
3, 15, 16	Si	677	1.0	9.25 ± 0.40	65.8 ± 1.6	26[a]	26
4	a-Si:C:H	260	1.0	9.30 ± 0.40	74.03 ± 2.6	18	18.5
5	a-Si:C:H	466	1.0	10.11 ± 0.49	76.6 ± 1.8	23[b]	22
6	a-Si:C:H	677	1.0	9.45 ± 0.37	74.7 ± 2.7	14.5	23
7	None	466	1.0	NA	NA	0	0
8	a-Si:C:H	466	5.0	11.14 ± 0.20	85.28 ± 1.26	14	9

[a]Film 3 failed at 6.5 N apparently owing to a pre-existing flaw. Failure of flaw-free film was observed microscopically at 26 N.
[b]Film 5 failed at 17 N apparently owing to a pre-existing flaw. Failure of flaw-free film was observed microscopically at 23 N.

deposited at an energy of 450 eV directly onto an M50 substrate without an intermediate layer. The arithmetic-average surface roughness R_a proved to be independent of accelerating energy during deposition and was determined to be 12 ± 3.8 nm for all DLC films.

Similarly, the surface microstructure was determined to be independent of deposition energy and was found to be essentially featureless. In contrast to the present study of DLC films deposited by ion-beam techniques, DLC films deposited by the PVD technique of saddle-field, fast atom beam (FAB) deposition exhibited microstructures consisting of small but well-defined spheres having diameters between 0.1 and 0.3 μm [20, 26].

3.2. Raman spectroscopy

The Raman spectrum from a solid is a result of inelastic scattering of optical photons by lattice vibrations and hence provides a method for probing the lattice dynamics. Owing to the nature of this interaction, Raman spectroscopy provides a sensitive method for monitoring changes in the solid that disrupt the translational symmetry of the solid. Raman spectroscopy has been used extensively in the study of disorder and crystallite formation in carbon materials [27–31]. Over the past decade, Raman spectra have been employed extensively to study the properties of amorphous carbon films (a-C and a-C:H), the properties of which can be varied from graphite-like to diamond-like. Recently, it has been shown that a wide range of physical properties of a-C can be correlated with subtle changes in the carbon π orbitals [32].

In graphite, only the E_{2g} modes of zone center optical phonons in graphite are Raman active; these occur at 42 and 1581 cm^{-1}. The graphite phonon density of states, however, exhibits maxima above and below the line at 1581 cm^{-1} (G). Phonons associated with these densities of states cannot be observed in single-crystal graphite owing to wave-vector conservation, but they are observed in disordered graphites, in which wave-vector conservation is relaxed owing to loss of long-range order in the crystal [33]. As disorder in the crystal increases, new features at 1360 and 1620 cm^{-1} emerge, commonly noted as D and D′ respectively, which are the so-called disorder-induced peaks. The Raman spectrum of an a-C:H film deposited from 260 eV ionized methane is shown in Fig. 1 and resembles those of i-C films reported by others.

The spectrum shown in Fig. 1 can be decomposed into three contributions as shown in the figure, with features centered at 1206, 1360, and 1536 cm^{-1}. A simple two-band model yields a fit which is inferior to the fit obtained using the three-band model. The shift in the G band to lower frequencies arises from the use of the laser excitation wavelength of 488.0 nm. As observed by

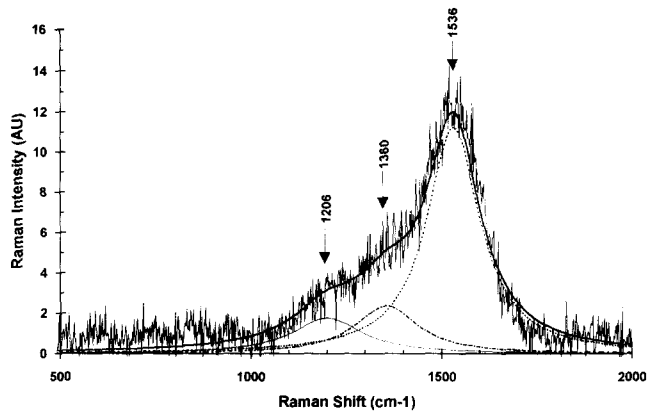

Fig. 1. Raman spectrum for film 4, deposited onto an amorphous Si:C:H interlayer from ionized CH_4 at an energy of 260 eV. The spectrum was excited using the 488.0 nm line of the Ar^+ ion laser. The best fit to the data was obtained using three spectral bands, as shown, centered at 1206, 1360, and 1536 cm^{-1}.

Wagner *et al.* [34], there is a shift in frequency of the G-band feature due to scattering from π-bonded clusters which is resonantly enhanced for photon energies approaching the π–π^* resonance of sp^2-bonded carbon. The band at 1360 cm^{-1} is in agreement with the disorder band seen in disordered graphites, while the band at 1206 cm^{-1} has been observed by others but not explicitly discussed. These three spectral features are common to all of the films that were deposited and measured as part of this study. Only small deviations in the Raman spectra have been observed as a result of variations in ion deposition energy over the range 260–677 eV.

3.3. IR reflectivity

The IR spectrum of diamond-like carbon has been used extensively as a means of obtaining detailed information about the C–H bonding configuration, the amount of hydrogen, and the ratio of sp^3 to sp^2 bonding in the films [35], although recently the validity of determination of the sp^3 to sp^2 ratio by IR absorption methods has been questioned [36]. In this study, the IR reflectivity has been used only to differentiate between relative amounts of sp^3 and sp^2 carbon-bonded hydrogen in the films. The IR reflectivity of two samples, deposited at ion energies of 450 and 650 eV, are shown in Fig. 2. The discrete absorption features are superimposed on an oscillating background which is due to constructive and destructive interference in the film thickness. The IR spectra of Fig. 2 are very similar to those reported by Dischler *et al.* [37]. Other researchers [28] have documented the presence of many features in the spectra of a-C films. For the present work, vibrational modes associated with C–H stretching occur in the 2800–3100 cm^{-1} region, and in the 700–1600 cm^{-1} region modes appear due to C–H deformation and C–C stretching. In Fig. 2, absorption features are detectable

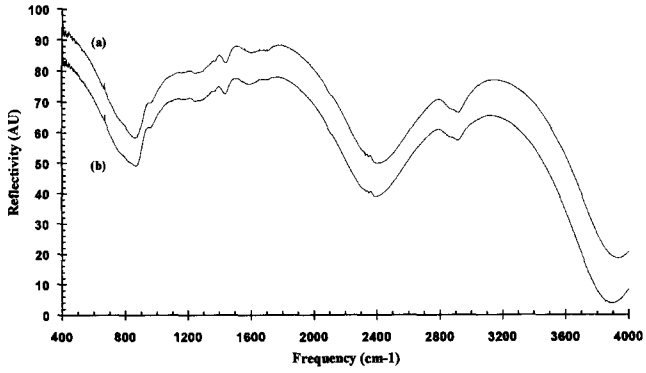

Fig. 2. IR reflectivity spectra of two films deposited at (a) 466 eV and (b) 677 eV. The spectra have been displaced arbitrarily in the vertical direction for clarity.

at around 780, 880, 960, 1250, 1300, 1360, 1430, 1600, 1700, 2855, 2920, 3000, and 3060 cm^{-1}. The spectra reported here differ somewhat from that reported by Dischler *et al.*, in that two broad absorptions may be noted at 1600 and 1700 cm^{-1}, whereas Dischler *et al.* reported features at 1570 and 1620 cm^{-1}. The authors cannot assign the observed band at 1700 cm^{-1}, but its presence has been noted in many of the films in the current study. In addition, no absorption has been observed at 1509 cm^{-1} in the current study. The most pronounced feature in this region of the spectrum is the absorption peak at 1430 cm^{-1}, which previously has been assigned to sp^2 C–C stretching.

In the 2700–3400 cm^{-1} region, absorption features appear due to C–H stretching modes. Figure 3 shows the C–H stretching region after the oscillatory background has been fitted and subtracted, leaving only the absorption features. This absorption band is composed of several different C–H stretching modes [28, 35]: sp^2 (aromatic) C–H stretch at 3060 cm^{-1}, sp^2 (olefinic) C–H stretch at 3000 cm^{-1}, sp^3 $C–H_3$ asymmetric stretch at 2970 cm^{-1}, sp^3 $C–H_2$ asymmetric stretch at 2920 cm^{-1}, sp^3 C–H stretch at 2920 cm^{-1}, sp^3 $C–H_3$ symmetric stretch at 2870 cm^{-1} [37], and sp^3 $C–H_2$ symmetric

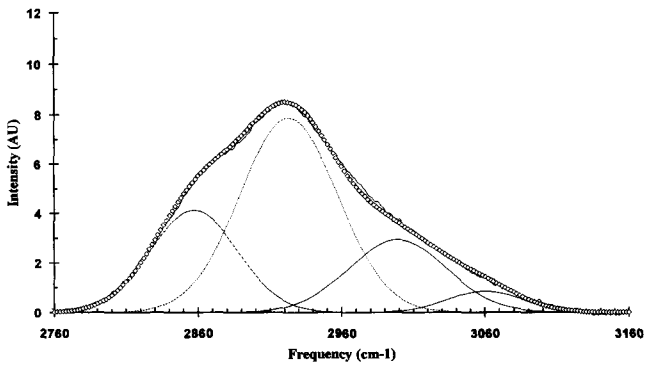

Fig. 3. Deconvolution of the C–H stretching region of film 5, which was deposited at 466 eV.

stretch at 2850 cm^{-1}. In addition, Dischler *et al.* [37] have reported a band at 3300 cm^{-1} due to sp^1 C–H stretch; this feature, however, has not been observed in the present study. The relative amounts of sp^3 and sp^2 carbon-bonded hydrogen can be calculated by fitting the absorption data and integrating the area under each absorption band. As shown in Fig. 3, most of the intensity falls in the bands at 2920 and 2855 cm^{-1}, peaks which are associated with sp^3-hybridized C–H bonds. The total intensity due to sp^2 carbon-bonded hydrogen is approximately 3.5 times smaller than that due to sp^3 carbon-bonded hydrogen. This was found to be the case for all of the films investigated, and no significant dependence has been noted for the relative amounts of sp^3 to sp^2 carbon-bonded hydrogen on the ion energy used during deposition except for films deposited at the highest energy of 677 eV.

The spectra for several films deposited at different ion energies over the a-Si:C:H interlayer were measured as part of this study; however, no significant differences among the films, except for minor variations in film thickness, were detectable from the IR spectra. In addition, the C–H stretching regions corrected for the oscillatory background were found to be very similar. The only exception is a slightly larger absorption intensity in the sp^2 region for the film deposited at 677 eV, for which the ratio of sp^3 to sp^2 carbon-bonded hydrogen is smaller than for the other films measured. This is in agreement with the trends reported by others on the onset of graphitization of a-C films by ion bombardment [38–40], for which the amount of sp^2 carbon-bonded hydrogen has been reported to increase with increasing ion energy; for the present study, however, the difference is small.

3.4. *Ultralow-load indentation*

The indentation and adhesion properties of the a-C:H films synthesized by broad-beam ion techniques are summarized in Table 1. Two observations are immediately obvious. First, little difference and no systematic dependence of nanoindentation properties on ion deposition energy emerge from examination of the data. As shown in the table, with two exceptions, all films studied exhibit hardness and elastic modulus values of 9.6 ± 0.5 GPa and 70 ± 5 GPa, respectively. For as-deposited, ultrahard films, this is well within the scatter normally associated with nanoindentation measurements [41, 42]. These values are, however, significantly lower than the range reported to apply to DLC coatings deposited by various techniques [43, 44]. Nonetheless, these lower hardness and stiffness measurements are consistent with the higher than normal percentage of sp^3-hybridized C–H bond types reported in Section 3.3, owing to the high degree of polymeric character for these a-C:H films and the relationship

which has been reported to exist between hardness and sp^3 concentration [45].

3.5. Adhesion

All deposition experiments resulted in the synthesis of adherent a-C:H coatings except for specimen numbers 1 and 7, the former of which was deposited onto an elemental Si interlayer at the lowest investigated beam energy of 266 eV and the latter of which was deposited at an energy of 450 eV directly onto an M50 substrate without an interlayer. For these two films, broad-beam deposition from ionized CH_4 failed to produce adherent a-C:H coatings, spalling spontaneously either immediately or within days following deposition.

Results from adhesion experiments for the remainder of the a-C:H films, as measured by the scratch technique, are summarized in Table 1. There appears to be a weak dependence of the critical load, as measured using light microscopy, L_c(LM), and as detected by the acoustic emission sensor, L_c(AE), on the ion beam energy during deposition. For example, the film which exhibits the highest critical load is film 15, which was deposited onto the elemental Si interlayer at the highest energy investigated, 677 eV.

Furthermore, it is clear that the adherence of the 5 μm film, specimen 8 shown in Fig. 4, is decidedly inferior to that of the films deposited to a thickness of approximately 1 μm for either interlayer composition. While stresses within the DLC films have not been determined for the current study, increases in intrinsic (growth) stresses for thicker a-C and a-C:H films [8–10] have been reported by other authors to result in adherence difficulties.

With the exception of the films which were deposited at 570 eV onto elemental Si interlayers, films 13 and 14, modest increases in adherence result from increases in deposition energy. For the films which were deposited onto the a-Si:C:H interlayer, the trend is less clear and less well defined; it appears, however, that an increase in deposition energy leads to slightly enhanced adherence for a-C:H films deposited onto a-Si:C:H interlayers, as well.

While the failures within the films are brittle in nature and display conchoidal fractures, as shown in Fig. 5 for film 4, both the M50 substrate and the film have undergone significant plastic deformation prior to failure of the coating. This observation is consistent with earlier observations [12, 13] that such films deposited using similar parameters onto M50 substrates undergo significant plastic deformation without spall formations during rolling contact fatigue experiments at a contact stress of 5.5 GPa.

The critical adhesion forces measured for these films are quite high for films of this type, especially considering that indicated critical forces as detected by both light microscopy and acoustic emission are values for incipient failure. In this respect, they are considerably more conservative than the criterion of continuous film failure, for example, as employed by Freller *et al.* [46]. Furthermore, the values are considerably greater in magnitude than those reported by Matthews and co-workers for a-C:H films deposited by thermionically assisted, electron-beam PVD [47] and FAB PVD [48] onto metallic and non-metallic substrates.

3.6. Sliding wear

For all deposition conditions, ball-on-disc experiments conducted at a sliding speed of 0.12 m s^{-1} produced

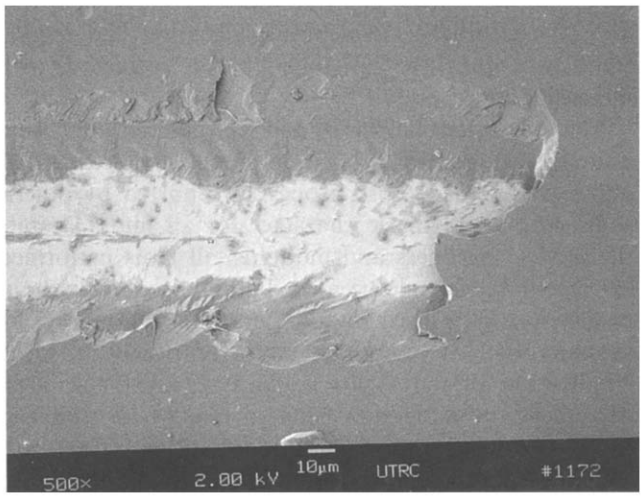

Fig. 4. Secondary electron image of film 8 (5 μm thick) deposited onto an a-Si:C:H interlayer at an energy of 466 eV. Stylus traverse direction is from left to right.

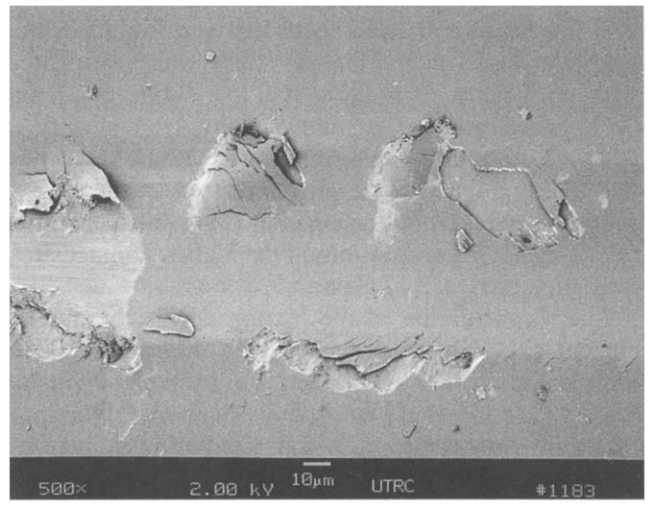

Fig. 5. Secondary electron image of film 4, deposited onto an a-Si:C:H interlayer at an energy of 260 eV. Stylus traverse direction is from left to right. The microstructure shows brittle, conchoidal fractures within and outside of the stylus path and plastic deformation within the film and the M50 substrate.

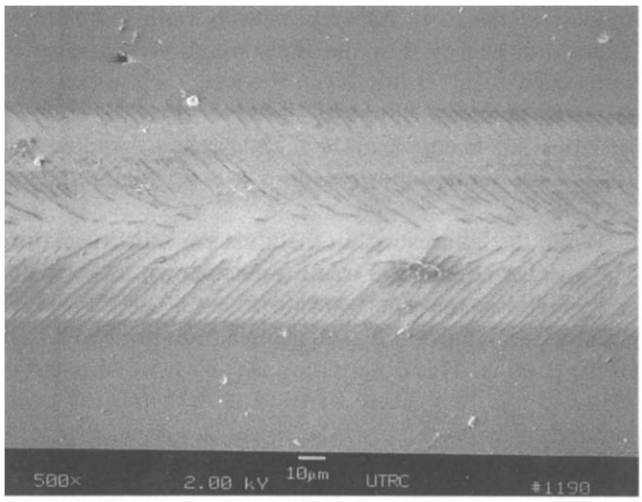

Fig. 6. Secondary electron image of film 15, deposited at an ion-beam energy of 677 eV onto an elemental Si interlayer. Stylus traverse direction is from left to right. Even at maximum stylus load applied, 30 N, this film exhibited only isolated spalling.

initial friction coefficients which ranged between 0.125 and 0.145. This behavior persisted essentially unchanged for all contact stress levels investigated with two exceptions. The film which was deposited at an energy of 677 eV (Fig. 6) showed a decrease in friction coefficient to a value of approximately 0.105, achieving this minimum at a contact stress level of 2.92 GPa and maintaining it through the 4800 disc rotations at the highest contact stress level investigated, 3.17 GPa. For the a-C:H film deposited at an energy of 350 eV, the friction coefficient remained relatively constant for contact stresses of 2.17 and 2.42 but increased to and saturated at approximately 0.15 for stress levels of 2.67 through 3.17 GPa. Indeed, a reasonably well-defined inverse relationship between friction coefficient and ion deposition energy emerged at the highest stress level investigated, with coefficients of friction of 0.153, 0.146, 0.127 and 0.106 being recorded for films which were deposited at 350, 467, 570 and 677 eV respectively. While the deposited films exhibited some surface distress in the form of scratches and minor abrasion, none were fully penetrated following 4800 disc rotations at the highest contact stress level investigated, 3.17 GPa.

The reconciliation of the friction coefficients for the current study to those reported by others for a-C:H films is unclear in some respects. For example, Pivin and Lee [49] found that "amorphous diamond" films produced by low-energy C^+ ion irradiation of various substrates exhibited significantly lower friction coefficients than films synthesized by means of laser-plasma PVD, suggesting that the finer scale of nodularity and smoother surfaces produced by the former technique were responsible. The friction coefficients for the current study are quite similar to those reported by Pivin and Lee for ion-irradiated substrates ($\mu \approx 0.12$); however, other authors have reported friction coefficients on the order of or less than 0.05, emphasizing the importance of transfer-layer formation [3–6, 50] or the transformation to graphite [2] for the achievement of low friction coefficients and/or wear rates. It is quite possible that, in addition to the explanations offered by others, the nature and composition of the counterface is of critical importance. The surface chemistry of the ruby sapphire balls used for the current investigation and their interaction with the deposited carbon films should be significantly different from those characteristics of metallic or alloy counterfaces; these differences are expected to affect the formation and/or retention of an a-C:H transfer layer.

4. Conclusions

Diamond-like (amorphous) carbon films have been deposited from ionized methane species at several different accelerating potentials, all of which have been observed to possess surfaces which are smooth and featureless. The films exhibited many of the characteristics of hydrogenated amorphous carbon, a-C:H. The Raman spectrum exhibited a very weak scattering signal with peaks at 1536, 1360 and 1206 cm^{-1}. The peaks at 1536 and 1360 cm^{-1} are characteristic of a-C films. The origin of the weaker feature at 1206 cm^{-1} is not presently understood. The IR spectra of the films showed many features in the 700–1700 cm^{-1} region associated with C–H deformation and C–C stretching vibrations. The films also showed an absorption in the 2800–3100 cm^{-1} region due to C–H stretching modes. The ratio of sp^3 to sp^2 carbon-bonded hydrogen in the films was found to be approximately 3.5 and did not show a strong dependence on the ion deposition energy. The general trend was that the sp^3-to-sp^2 ratio decreased with increasing ion energy.

The measured hardness and elastic modulus were quite independent of deposition energy and were softer and less stiff than those properties reported by others, suggesting a polymeric character for all films. Despite the modest hardness and modulus, all films performed extremely well in unlubricated sliding, surviving without penetration 4800 disc rotations against a stationary ruby sapphire ball at a contact stress of nearly 3.2 GPa. Application of the stylus method revealed a modest dependence of adherence between the a-C:H film and M50 substrate on ion deposition energy. The most superior adherence was exhibited by film 15, deposited at the highest energy of 677 eV onto an elemental Si interlayer, which survived applied stylus loads of 30 N with only isolated film failures.

Acknowledgment

The authors are pleased to acknowledge the experimental contributions of D. M. Sanford, R. M. Brown, and L. F. Conopask.

References

1 J. Robertson, *Diamond Relat. Mater., 1* (1992) 397.
2 K. Enke, *Thin Solid Films, 80* (1981) 227.
3 A. Erdemir, F. A. Nichols, X. Z. Pan, R. Wei and P. J. Wilbur, *Diamond Relat. Mater., 3* (1993) 119.
4 D. S. Kim, T. E. Fischer and B. Gallois, *Surf. Coat. Technol., 49* (1991) 537.
5 J.-P. Hirvonen, R. Lappalainen, J. Koskinen, A. Anttila, T. R. Jervis and M. Trkula, *J. Mater. Res., 5* (1990) 2524.
6 R. Memming, H. J. Tolle and P. E. Wierenge, *Thin Solid Films, 143* (1986) 31.
7 K. Miyoshi, *Surf. Coat. Technol., 44* (1990) 799.
8 K. Enke, H. Dimigen and H. Hubsch, *Appl. Phys. Lett., 36* (1980) 291.
9 A. Grill and V. Patel, *Diamond Relat. Mater., 2* (1993) 597.
10 C. Weissmantel, K. Bewilogua, K. Breuer D. Dietrich, U. Ebersbach, H. J. Erler, B. Rau and G. Reisse, *Thin Solid Films, 96* (1982) 31.
11 A. Grill, B. S. Meyerson and V. Patel, *Proc. Soc. Photo-Opt. Instrum. Eng., 969* (1989) 52.
12 R. Wei, P. J. Wilbur and M.-J. Liston, *Diamond Relat. Mater., 2* (1993) 898.
13 R. Wei, P. J. Wilbur, M.-J. Liston and G. Lux, *Wear, 162–164* (1993) 558.
14 R. Wei, P. J. Wilbur, A. Erdemir and F. M. Kustas, *Surf. Coat. Technol., 51* (1992) 139.
15 L. G. Tsinzerling, E. S. Berkovich, L. A. Sysoer and M. P. Shaskol'skaya, *Sov. Phys. Crystallogr., 14* (1970) 897.
16 M. J. Mayo, R. W. Siegel, A. Narayanaswamy and W. D. Nix, *J. Mater. Res., 5* (1990) 1073.
17 J. D. J. Ross, H. M. Pollock, J. C. Pivin and J. Takadoum, *Thin Solid Films, 148* (1987) 171.
18 C. Feldman, F. Ordway and J. Bernstein, *J. Vac. Sci. Technol. A, 8* (1990) 117.
19 M. F. Doerner and W. D. Nix, *J. Mater. Res., 1* (1986) 601.
20 C. V. Cooper, P. Holiday and A. Matthews, *Surf. Coat. Technol.*, in press.
21 C. Julia-Schmutz and H. E. Hintermann, *Surf. Coat. Technol., 48* (1991) 1.
22 H. Hintermann, *J. Vac. Sci. Technol. B, 2* (1984) 816.
23 P. A. Steinmann, Y. Tardy and H. E. Hintermann, *Thin Solid Films, 154* (1987) 333.
24 R. D. Arnell and I. Efeoglu, *Vacuum, 44* (1993) 805.
25 R. Wei, P. J. Wilbur, W. S. Sampath, D. L. Williamson, Y. Qu and L. Wang, *J. Tribol., 112* (1990) 27.
26 J. Smith, P. Holiday and A. Matthews, *Diamond Relat. Mater., 1* (1992) 355.
27 K. Nakamura, M. Fujitsuka and M. Kitajima, *Phys. Rev., B, 41* (1990) 12260.
28 J. Robertson, *Adv. Phys., 35* (1986) 317.
29 H. Tsai and D. B. Bogy, *J. Vac. Sci. Technol. A,5* (1987) 3287 (1987).
30 J. C. Angus and C. C. Hayman, *Science, 241* (1988) 913.
31 R. Messier, A. R. Badzian, T. Badzian, K. E. Spear, P. Bachmann and R. Roy, *Thin Solid Films, 153* (1987) 1.
32 C. Gao, Y. Y. Wang, A. L. Ritter and J. R. Dennison, *Phys. Rev. Lett., 62* (1989) 945.
33 R. J. Nemanich and S. A. Solin, *Phys. Rev. B, 20* (1978) 392.
34 J. Wagner, M. Ramsteiner, Ch. Wild and P. Koidl, *Phys. Rev. B, 40* (1989) 1817.
35 J. W. Zou, K. Schmidt, K. Reichelt and B. Dischler, *J. Appl. Phys., 67* (1990) 487.
36 M. A. Tamor and C. H. Wu, *J. Appl. Phys., 67* (1990) 1007.
37 B. Dischler, G. Brandt and P. Koidl, *Appl. Phys. Lett., 42* (1983) 636.
38 K. Bewilogua, D. Dietrich, L. Pagel, S. Schurer and C. Weissmantel, *Surf. Sci., 86* (1979) 308.
39 C. Weissmantel, *Thin Solid Films, 58* (1979) 101.
40 T. Mori and Y. Namba, *J. Vac. Sci. Technol. A, 1* (1983) 23.
41 C. P. Beetz, Jr., C. V. Cooper and T. A. Perry, *J. Mater. Res., 5* (1990) 2555.
42 C. V. Cooper and C. P. Beetz, Jr., *Surf. Coat. Technol., 47* (1991) 375.
43 F. Demichelis, C. F. Pirri, A. Tagliaferro, G. Benadetto, L. Boarino, R. Spagnolo, E. Dunlop, G. Haupt and W. Gissler, *Diamond Relat. Mater., 2* (1993) 890.
44 P. J. Martin S. W. Filipczuk, R. P. Netterfield, J. S. Field, D. F. Whitnall and D. R. McKenzie, *J. Mater. Sci. Lett., 7* (1988) 410.
45 M. A. Tamor, W. C. Vassell and R. C. Carduner, *Appl. Phys. Lett., 58* (1991) 592.
46 H. Freller, H. Hempel, J. Lilge and H. P. Lorenz, *Diamond Relat. Mater., 1* (1992) 563.
47 A. Dehbi-Alaoui, A. Matthews and J. Franks, *Surf. Coat. Technol., 47* (1991) 722.
48 P. Holiday, A. Dehbi-Alaoui and A. Matthews, *Surf. Coat. Technol., 47* (1991) 315.
49 J. C. Pivin and T. J. Lee, *Diamond Relat. Mater., 1* (1992) 650.
50 J. Meneve, E. Dekempeneer, R. Jacobs, L. Eersels, V. Van Den Bergh and J. Smeets, *Diamond Relat. Mater., 1* (1992) 553.